O-Acetylation of Cryptococcal Capsular Glucuronoxylomannan Is Essential for Interference with Neutrophil Migration[1]

Pauline M. Ellerbroek,[2]*[†] Dirk J. Lefeber,[2]*[†] Richard van Veghel,[‡] Jelle Scharringa,*[†] Ellen Brouwer,*[†] Gerrit J. Gerwig,[§] Guilhem Janbon,[¶] Andy I. M. Hoepelman,*[†] and Frank E. J. Coenjaerts[3]*[†]

The capsular polysaccharide glucuronoxylomannan (GXM) of *Cryptococcus neoformans* has been shown to interfere with neutrophil migration. Although several receptors have been implied to mediate this process, the structural perspectives are unknown. Here, we assess the contribution of 6-*O*-acetylation and xylose substitution of the $(1\rightarrow3)$-α-D-mannan backbone of GXM, the variable structural features of GXM, to the interference with neutrophil migration. We compare chemically deacetylated GXM and acetyl- or xylose-deficient GXM from genetically modified strains with wild-type GXM in their ability to inhibit the different phases of neutrophil migration. Additionally, we verify the effects of de-*O*-acetylation on neutrophil migration in vivo. De-*O*-acetylation caused a dramatic reduction of the inhibitory capacity of GXM in the in vitro assays for neutrophil chemokinesis, rolling on E-selectin and firm adhesion to endothelium. Genetic removal of xylose only marginally reduced the ability of GXM to reduce firm adhesion. In vivo, chemical deacetylation of GXM significantly reduced its ability to interfere with neutrophil recruitment in a model of myocardial ischemia (65% reduction vs a nonsignificant reduction in tissue myeloperoxidase, respectively). Our findings indicate that 6-*O*-acetylated mannose of GXM is a crucial motive for the inhibition of neutrophil recruitment. *The Journal of Immunology,* 2004, 173: 7513–7520.

T he pathogenic fungus *Cryptococcus neoformans* mainly causes serious infections in the immunocompromised host, such as AIDS patients. The cryptococcal polysaccharide capsule has been recognized as a crucial virulence factor. Its main component is the polysaccharide glucuronoxylomannan (GXM),[4] which is abundantly shed into its surroundings and can be detected in body fluids of patients during infection (1, 2). High serum titers of GXM during cryptococcosis have been associated with progressive disease and subdued inflammatory responses (1, 3). It has previously been recognized that GXM exerts various effects on the immune apparatus of the host, such as interference with phagocytosis (4), activation of the complement system (5), suppression of T cell-mediated immunity (6), and up-regulation of cytokine production (7, 8). Moreover, in vitro as well as in vivo, GXM has been shown to interfere with the migration of leukocytes toward chemotactic stimuli and inflammatory sites (9–14), and different mechanisms contribute to this phenomenon. First, cryptococcal GXM impairs neutrophil migration toward chemoattrac-

tants (10, 11, 14), despite adequate stimulation of chemokine production (8, 11, 15). A combination of the intrinsic chemoattracting properties of circulating GXM (10, 16) and down-regulation of chemokine receptors (17) will prevent leukocytes from leaving the bloodstream and migrating toward inflammatory sites. Second, polysaccharides interfere with leukocyte adhesion to the endothelium. GXM has been demonstrated to induce L-selectin shedding (14, 18), to bind CD18 (19), and to actually impair both phases of neutrophil adhesion to the endothelium, namely the initial rolling (20) as well as subsequent firm binding to the endothelium (21).

Although several potential cellular receptors for GXM have been recognized (i.e., CD14, TLR4, and CD18 (19)), the mechanism by which GXM modulates neutrophil migration remains to be elucidated. From a structural perspective, nothing is known about the epitopes of GXM responsible for its capacity to inhibit neutrophil migration.

GXM consists of a linear $(1\rightarrow3)$-α-D-mannan backbone that is variably *O*-acetylated and substituted with glucuronic acid and variable amounts of xylose. The importance of *O*-acetylation and xylose for other immunological effects of GXM has mainly been studied using different cryptococcal serotypes and naturally prevailing capsule variations (22–25). Additionally, chemical modification of GXM (25–27) and, more recently, the identification of the genes involved in *O*-acetylation (*CAS1*, encoding for a putative glycosyl transferase) and the synthesis of UDP-xylose (*UXS1*, encoding for UDP-xylose synthase) (28–30) have provided more knowledge of their relevance for the function of GXM (31). For instance, *O*-acetyl has been recognized as the major epitope for recognition of GXM by various monoclonal and polyclonal Abs (22, 27, 31, 32) and as important for clearance of GXM from serum (31). Xylose has been shown to play a role in complement deposition on cryptococci and accumulation of GXM in the spleen (31, 33, 34). Neither xylose nor *O*-acetyl appeared to play a role in the inhibition of phagocytosis by GXM in vitro (26, 31). Finally, glucuronyl side-chains provide a negative cellular charge to GXM,

and thus far, modification by decarboxylation has not revealed other functions (26, 35, 36).

In this study, we investigate the importance of O-acetylation and xylose for the interference with neutrophil migration. We compare chemically deacetylated GXM and O-acetyl- or xylose-deficient GXM from cas1Δ and uxs1Δ mutant strains, respectively, with wild-type GXM in their ability to inhibit in vitro neutrophil chemokinesis, rolling, and adhesion to the endothelium. Furthermore, we investigate the impact of deacetylation on neutrophil influx in a rat model of myocardial ischemia, in which we recently established that GXM treatment diminishes neutrophil influx in the injured tissues (37).

Materials and Methods

Cryptococcal strains

The strains used in this study are described in Table I. The strains lacking xylose (NE178) or O-acetylation (NE168) (29, 30) were obtained by back-crossing the disrupted strain with the original strain (JEC155, MATα ura5 ade2 and JEC156, MATa ura5 ade2, respectively; serotype D) (38). NE167 was used as an isogenic control 29. C. neoformans serotype A (ATCC-62066) was obtained from the American Type Culture Collection (Manassas, VA). Pneumococcal polysaccharide (PnPS type 3) was a kind gift of H. Snippe (Eijkman Winkler Institute, University Medical Center Utrecht, The Netherlands) (39).

Isolation and deacetylation of GXM

GXM was isolated from the various strains as previously described (40). Briefly, C. neoformans was grown in a chemically defined broth for 5 days followed by autoclaving. The polysaccharides present in the medium were precipitated with calcium acetate and ethanol. After dissolving the polysaccharides in sodium chloride solution and brief sonication by ultrasound, GXM was precipitated by differential complexation with hexadecyltrimethylammonium bromide (Sigma-Aldrich, St. Louis, MO). Isolated GXM was again precipitated with ethanol, then dissolved and sonicated for 2 h, followed by centrifugation and dialysis. Finally, GXM was recovered by lyophilization, dissolved in PBS (5 mg/ml), sterilized by filtration, and stored at −20°C.

GXM from ATCC-62066 was deacetylated by incubating GXM at 5 mg/ml in aqueous NaOH at pH 11 for 24 h. After neutralization with aqueous HCl, the solution was dialyzed against bi-distilled water and lyophilized.

Chemical and physical properties of GXM

Acetyl group determination was performed according to Hestrin (41) using acetylcholine as a standard. The acetyl content of GXM preparations was expressed relative to that of GXM derived from ATCC-62066 (serotype A), which contained an average of two acetyl groups per three mannose residues, as determined by nuclear magnetic resonance ([^{1}H]NMR) spectroscopy at 500 MHz in D_2O.

Rheological measurements were performed on an MCR300 modular compact rheometer (Physica Messtechnik, Ostfildern, Germany) using a cone-plate geometry of stainless steel with a diameter of 50 mm and a cone angle of 2°. Results were obtained using a rotation test and are expressed as viscosity (η) in mPa · s.

For monosaccharide analysis, samples were subjected to methanolysis (1.0 M methanolic HCl, at 85°C for 24 h, followed by trimethylsilylation (5:1:1 pyridine:chlorotrimethylsilane:hexamethyldisilazane) at room temperature for 30 min) and analyzed by gas chromatography (GC) and GC-mass spectrometry (42). Molecular mass distribution of GXM was determined by gel filtration chromatography of 1 mg/ml GXM samples (Superose 6.0 column; Pharmacia, Peapack, NJ) as previously described (21).

The structures of the GXM isolated from strains NE167, NE168, and NE178 were determined by [^{1}H]NMR spectroscopy as reported previously (29, 30). Comparison of the chemical shifts of the wt strain with those of uxs1Δ strain indicated that the absence of the (1→2)-β-D-xylopyranosyl residue is the only change. Comparison of NMR data from strains NE168 vs NE167 showed that the only change was a complete absence of O-acetylation in the de-O-acetylated strain (NE168).

Maintenance of endotoxin-free conditions

All materials were kept under pyrogen-free conditions. Stock solutions (5 mg/ml) of the various types of GXM were tested for the presence of Endotoxin using a Limulus amebocyte lysate assay (Coatest Endotoxin Diagnostica, Mölndal, Sweden). The detected LPS concentration was always <0.6 ng/ml; LPS contents actually present in the neutrophil assays described in this paper thus never exceeded 30 pg/ml.

Cells and cell lines

Primary HUVECs were isolated from donor umbilical veins according to the method described by Jaffe et al. (43) and were cultured in commercial Endothelial Growth Medium (EGM-2; Cambrex, Walkersville, MD). Only passages 1 and 2 were used for the experiments. Chinese hamster ovary (CHO) cells stably transfected with human E-selectin (44) were kindly provided by R.C. Fuhlbrigge (Department of Dermatology, Brigham and Women's Hospital, Boston, MA) and originated from R. Lobb (Biogen, Cambridge, MA). The cells were cultured in Modified Eagle's Medium (Invitrogen Life Technologies, Breda, The Netherlands) containing 10% FCS (v/v) and penicillin/streptomycin. CHO cell monolayers were grown to confluence in 3–4 days on plastic cover slips before flow experiments.

Isolation and GXM treatment of human neutrophils

Human neutrophils were isolated from healthy volunteers as previously described (21). Isolated neutrophils were suspended in sterile RPMI 1640/human serum albumin (HSA) (static adherence assays), HBSS/HSA (chemotaxis assay), or HEPES buffer (rolling experiments) at 2×10^6 cells/ml. HEPES buffer contained 20 mM HEPES, 132 mM NaCl, 6 mM KCl, 1 mM $MgSO_4$, 1.2 mM KH_2PO_4 supplemented with 5 mM glucose, 1.0 mM $CaCl_2$, and 0.5% (v/v) HSA.

Based on the results of previous studies and dose/response curves, the conditions of GXM treatment of neutrophils (i.e., duration, GXM concentration, and temperature) differed among the various assays (20, 21). Before the static adherence assay, neutrophils were incubated at 37°C with 0.1–1 μg/ml GXM for 45 min, at which maximal inhibition was detected previously (21). Before the rolling experiments, the neutrophils were treated with 10 μg/ml GXM (room temperature, 30 min). For the chemotaxis assay, a dose-response curve was performed for the two unmodified types of GXM. For GXM derived from ATCC-62066, the optimal inhibiting concentration was 250 μg/ml (room temperature, 30 min), whereas for GXM derived from NE167, optimal inhibition required a concentration of 100 μg/ml.

Static adhesion assay

Static adhesion assays were performed as previously described (21). HUVECs were plated on fibronectin-coated NUNC 72-well plates (Invitrogen Life Technologies) and grown to confluence in 1–2 days. After stimulation with 10 ng/ml TNF-α (Roche, Almere, The Netherlands) at 37°C for 6 h, the untreated (control) or GXM-treated neutrophils were added to the wells in a concentration of 10^6/ml (neutrophil:endothelial cell ratio = 5:1) and were left to adhere at 37°C for 15 min. The endothelium was then carefully washed and the adherent cells were fixed with 2% paraformaldehyde (pH 7.4). Adherent cells were counted within a fixed frame of 1 mm² in the center of each well by fluorescence microscopy (Leitz Fluovert inverted microscope; Leitz/Leica, Bensheim, Germany). Measurements were performed in quadruple wells for each variable. All tests were repeated using different batches of donor cells.

Table I. *C. neoformans strains used in this study*

Strains	Genotype	Serotype	Capsule Modification	Source or Reference
NE167	MATα CAS1 UXS1	D	–	Refs. 29 and 31
NE168	MATα cas1Δ::ADE2	D	O-acetyl deficient	Refs. 29 and 31
NE178	MATa uxs1Δ::ADE2	D	Xylose deficient	Refs. 30 and 31
ATCC-62066	Unknown	A. chemotype 5	–	American Type Culture Collection

Chemotaxis assay

Neutrophils were labeled with 5 μg/ml Calcein-AM (Molecular Probes, Eugene, OR) at room temperature for 30 min. After washing, the neutrophils were incubated with the different types of GXM for another 30 min. Migration (45) was measured using 96-well microchambers with polycarbonate filters (ChemoTx; NeuroProbe, Gaithersburg, MD). To each bottom well, 29 μl of HBSS (negative control) or 29 μl of the chemotactic factor fMLP was added (1 nM; Sigma-Aldrich). Polycarbonate filters with an 8-μm pore size (ChemoTx; NeuroProbe) were placed on top of the plate, and 25 μl of neutrophil suspension (2.5×10^6 cells/ml in HBSS/HSA) was directly placed onto the hydrophobic filter sides. After incubation for 45 min (37°C, 5% CO$_2$), the nonmigrating cells were gently flushed off the filter with PBS and the cells that migrated into the filter and the bottom chamber were determined by measuring the fluorescence in a multiwell fluorescence plate reader (excitation, 485 nm; emission, 530 nm; Flexstation; Molecular Devices, Sunnyvale, CA). Control wells containing Calcein-labeled cells were included to obtain the maximum fluorescence value.

Perfusion experiment and analysis

Perfusions under steady flow conditions were performed in a modified form of a transparent parallel plate perfusion chamber (20, 46). The perfusion chamber contains a circular plug on which cover slips (18 × 18 mm) coated with E-selectin-expressing CHO cells were placed and exposed to neutrophil suspensions in HEPES buffer. For each individual perfusion, 1.2 ml of neutrophil suspension (2.10^6/ml) was aspirated from a reservoir through plastic tubing through the perfusion chamber with a Harvard syringe pump (Harvard Apparatus, South Natick, MA), by which the flow rate could be precisely controlled. In individual experiments, the neutrophils were perfused through the chamber at 37°C and at a wall shear stress of 3.0 dynes/cm^2. During perfusions, the flow chamber was mounted on a microscope stage (DM RXE; Leica, Weitzlar, Germany), which was equipped with a black and white charge-coupled device video camera (Sanyo, Osaka, Japan), coupled to a VHS video recorder. Perfusions were recorded on videotape and video images were evaluated for the number of cells in close contact with the E-selectin CHO cells (that is, adherent cells) using dedicated routines made in the image analysis software Optimas 6.1 (Media Cybernetics Systems, Silver Spring, MD). Neutrophils in contact with the surface, which consisted of both rolling cells and firmly adhered cells (from now on together referred to as "adherent cells"), appeared as bright white-centered cells after proper adjustment of the microscope during recording. The adherent cells were detected by the image analyzer. The number of adherent neutrophils was measured after 5-min perfusion at a minimum of 25 high-power fields (total surface of at least 1 mm^2).

Animals

Male Wistar rats (Harlan, Zeist, The Netherlands) weighing 280–320 g were housed according to standard procedures. The experimental procedures were approved by the Ethical Committee for the Use of Experimental Animals within the University Medical Center Utrecht.

Experimental protocol of myocardial ischemia/reperfusion injury

Rats were subjected to either coronary artery ligation or a sham operation, according to the method of Fishbein et al. (47). Briefly, after anesthetizing with urethane and initiation of mechanical ventilation, the thorax was opened and a silk (6–0) suture was looped under the left descending coronary artery near the origin of the pulmonary artery. In infarct animals, the coronary artery ligature was closed; in sham animals, the suture was not closed. A bolus of 250 μl of normal saline (placebo) or 2.5 mg GXM dissolved in 250 μl of normal saline was administered i.v. to rats 15 min after coronary occlusion. After a 1-h period of occlusion, the circulation of the coronary artery was restored by opening the suture. The early influx of neutrophils reaches their peak 2–6 h after restoration of the blood flow of ischemic myocardium (48, 49). Hence, after a 3-h period of reperfusion, the rats were deeply anesthetized with urethane, and the hearts were quickly excised and processed for determination of the neutrophil influx in the ischemic area. Blood was collected from the vena cava in plastic tubes without anticoagulant and in tubes containing sodium heparin just before the heart was isolated. The blood was centrifuged immediately in a refrigerated centrifuge at 2100 × g. Plasma and serum were collected and stored at −70°C.

Determination of the ischemic area

The coronary arteries of the excised hearts were perfused with cold PBS by infusion of the aorta. The nonperfused area (ischemic region; area at risk) was determined by closing the suture again and then perfusion of the isolated heart with trypan blue. As a result, the perfused area was stained blue, whereas the nonperfused area (ischemic area) remained unstained. This area was separated and deeply frozen for later myeloperoxidase (MPO) measurements.

Quantification of neutrophil infiltration

MPO activity was used as a marker of tissue infiltration by neutrophils (50, 51), and detection was based on its ability to degrade hydrogen peroxide. MPO was extracted from the cardiac tissues according to the method described by Bradley et al. (52). The dissected ischemic areas were rapidly frozen in liquid nitrogen, pulverized, and weighed. The material was homogenized in 0.5% hexadecyltrimethylammonium bromide (Sigma-Aldrich) in 50 mM potassium phosphate buffer, pH 6.0, to provide a 10% homogenate (w/v), followed by sonication on ice and three freeze-thaw cycles. After centrifugation at 25,000 × g, the resulting supernatants were chromatographed on 1 ml of Sephadex G-75 columns (Pharmacia Biotech, Uppsala, Sweden) to separate MPO from tissue myoglobin and vascular hemoglobin that may affect the MPO assay (50). The second effluent with the size of the void volume was collected and assayed. The MPO activity was determined by mixing 50 μl of sample with 1.45 ml of 50 mM potassium phosphate buffer containing 0.167 mg/ml o-dianisidine hydrochloride (Sigma-Aldrich). After the addition of hydrogen peroxide (final concentration of 0.0005%), the change in absorbance at 460 nm was measured spectrophotometrically every 15 s for 5 min (Genesys 10 UV; Thermo Spectronic, Rochester, NY). The MPO activity was expressed as the change in absorbance per minute per 100 mg of heart tissue.

GXM detection in sera

GXM was determined in serum by the Premier Cryptococcal Ag ELISA (Meridian Bioscience Europe, Heusden/Destelbergen, Belgium) (12). A standard concentration curve was created by reducing the absorbance data from dilution series of GXM in rat serum by computer software capable of generating a four-parameter logistic curve fit.

Activation of complement in rat plasma

Complement activation by GXM was achieved by mixing 45 μl of plasma with 5 μl of GXM diluted in PBS to achieve final GXM concentrations ranging between 10 μg/ml and 1 mg/ml. The positive control consisted of rat plasma stimulated with 15 mg/ml Zymosan at 37°C for 1 h, which is a potent inducer of the alternative complement pathway (53).

Detection of C5a in plasma

Undifferentiated U937 cells stably transfected with the human receptor for C5a (U937-C5aR) were a kind gift from E. R. Prossnitz (Department of Pathology, State University of New York, New York, NY) (54). The U937-C5aR cells were loaded with a calcium-specific intracellular probe (fluo-3-acetoxymethyl ester; room temperature, 20 min) in RPMI 1640 containing 0.1% HSA (55). C5a has been shown to induce a rapid and transient increase in free intracellular calcium concentration in the U937-C5aR cells, which correlates with an increase in fluo-3-acetoxymethyl ester fluorescence signal as measured by flowcytometry (at 530 nm; FACS) (54, 55). After washing, the fluorescence of each sample of cells (180 μl of cells at 10^6/ml) was first measured to determine the basal calcium level. Then, 20 μl of rat plasma was added followed by repetitive measurements during 10 s. For each determination, the response was taken as the peak fluorescence occurring within 10 s of ligand addition.

Statistics

All data were analyzed by a univariate ANOVA test using a two-factor ANOVA, analyzing only main effects (in which the donor was set as a blocking factor). To compare multiple treatment groups to each other or to the control, the ANOVA was then followed by a post hoc analysis by Bonferroni's test. Any p values < 0.05 were considered significant.

Results

Chemical and physical aspects of GXM

The acetyl content and monosaccharide analysis of unmodified GXM and chemically and genetically modulated GXM are presented in Table II. Chemical analyses confirmed the integrity of all preparations used in this study. Chemical deacetylation of GXM of strain ATCC-62066 did not change the monosaccharide ratio. The mannose and glucuronic acid ratios of all types of GXM did not differ significantly. Strain NE178 lacked the *UXS1* gene encoding for UDP-xylose synthase, and consequently GXM derived from this strain contained no detectable amount of xylose.

Table II. *Monosaccharide and O-acetyl analysis of GXM[a]*

Strain	Man	Xyl	GlcA	% Ac
GXM ATCC-62066	3.9	2.2	1.0	100
GXM ATCC-62066: De-O-Ac	3.7	2.2	1.0	<5
NE-167	3.6	1.1	1.0	60
NE-168 (*cas1*Δ)	3.6	1.9	1.0	9
NE-178 (*usx1*Δ)	3.5	–	1.0	81

[a] Acetyl group determination was performed according to Hestrin (41) using acetylcholine as a standard. The acetyl content of GXM preparations is expressed relative to that of GXM derived from ATCC-62066, which contains an average of two acetyl groups per three mannose residues as determined by ^{1}H NMR spectroscopy at 500 MHz in D_2O. For monosaccharide analysis, samples were subjected to methanolysis, followed by trimethylsilylation, and were analyzed by GC and GC-mass spectrometry (42). The different monosaccharide contents are expressed as molar ratios of mannose to xylose to glucuronic acid.

Corresponding with earlier reports (56), unmodified GXM of the serotype D strain (NE167) had a lower *O*-acetyl content (60%) when compared with that of the serotype A strain (ATCC-62066).

The acetyl content of chemically deacetylated GXM of strain ATCC-62066 and the *O*-acetyl-negative *cas1*Δ strain (NE168) was <5% and 9%, respectively (Table II). In general, the ratio of mannose:xylose:glucuronic acid varies between 3:1:1 and 3:4:1, depending on the strain (56). Here, the isogenic control NE167 strain (serotype D) had a relatively low xylose content compared with all other types of GXM (Table II).

Rheological measurements showed no difference in viscosity between GXM and chemically deacetylated GXM at both concentrations and temperatures tested. Moreover, the Molecular mass ranges were identical as determined by gel filtration chromatography, i.e., elution curves were identically shaped (21) and ranged between 100 and 1500 kDa (data not shown).

O-*acetylation of GXM is required for interference with chemokinesis of neutrophils*

In vitro, GXM treatment of neutrophils has been shown to inhibit the chemokinesis of neutrophils toward various chemoattractants such as IL-8, platelet-activating factor, C5a, and fMLP (9–11, 14). To assess the importance of *O*-acetyl or xylose for this function of GXM, we compared the effect of intact GXM with that of GXM lacking *O*-acetylation or xylose in a chemotaxis assay.

In our chemotaxis assay, preincubation of neutrophils with unmodified GXM derived from strain ATCC-62066 inhibited the chemokinesis of neutrophils toward fMLP by 34% (Fig. 1; $p < 0.05$), whereas chemically deacetylated GXM from this strain did not affect chemokinesis significantly (inhibition 9%, $p = 0.24$; $p < 0.05$ when compared with unmodified GXM). Similarly, *O*-acetyl-positive GXM derived from strain NE167 blocked neutrophil migration by 46% ($p < 0.05$), whereas GXM deficient in *O*-acetylation (from the isogenic *cas1*Δ strain NE168) was considerably less potent (inhibition 19%, $p < 0.05$ when comparing with untreated neutrophils and with treatment by *O*-acetyl-positive GXM). GXM lacking xylose from the *uxs1*Δ strain (NE178) blocked neutrophil migration toward fMLP by 38%, which did not differ significantly from the inhibition caused by xylose-positive GXM from the isogenic strain NE167.

Therefore, we conclude that *O*-acetylation of GXM, but not xylose, is necessary for its ability to interfere with neutrophil chemokinesis.

O-*Acetylation of GXM is important for its ability to inhibit neutrophil rolling*

We previously reported that GXM impairs the rolling of neutrophils on stimulated endothelium as well as on E-selectin-expressing CHO cells (20). In the current study, we chose to flow the neutrophils over monolayers of E-selectin-transfected CHO cells
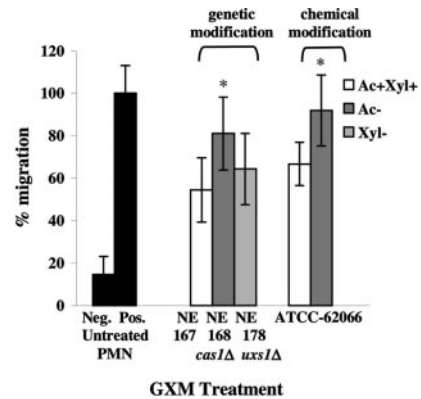

FIGURE 1. Chemotaxis of GXM-treated neutrophils toward fMLP. Neutrophils were treated with medium (no treatment) or GXM (GXM from NE strains at 100 µg/ml; GXM from ATCC-62066 at 250 µg/ml, room temperature, 45 min), and their chemokinesis toward fMLP was compared in a chemotaxis assay. The cells that migrated into the filter and the bottom chamber were determined by measuring the fluorescence in a multiwell fluorescence plate reader. Observations were made in triplicate. Results are the average of 11 experiments and migration is expressed as a percentage of the migration of untreated neutrophils (positive control, 100%). Negative control, Chemokinesis of untreated control toward PBS; positive control, chemokinesis of untreated control toward fMLP; Ac^+Xyl^+, GXM containing acetyl and xylose; Ac^- or Xyl^-, acetyl- or xylose-deficient GXM, respectively. *, $p < 0.05$ when comparing the chemokinesis of modified GXM with that of neutrophils treated with unmodified GXM. The error bars represent the SDs.

rather than over stimulated endothelium, because it provided us with a more selective rolling model in which firm binding between integrins and their ligands is minimized.

Here, both types of intact GXM derived from the ATCC-62066 and from strain NE167 reduced neutrophil rolling on E-selectin by 40% and 32%, respectively (Fig. 2; $p < 0.05$ for both treatments).
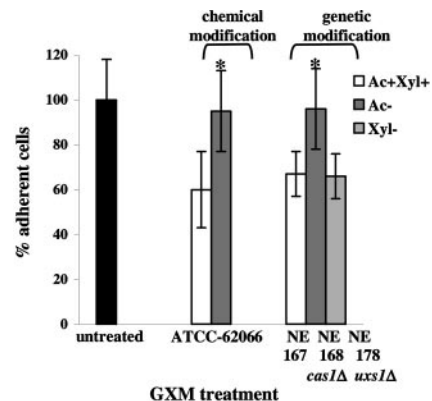

FIGURE 2. Rolling of GXM-treated neutrophils on E-selectin transfectants. Neutrophils were incubated with buffer (no treatment) or different types of GXM (10 µg/ml, room temperature, 30 min) and subsequently flown over E-selectin-expressing CHO cells (see *Materials and Methods*). Cells were allowed to interact with the endothelium for 5 min followed by video capturing of images. For each flow, the numbers of rolling (adherent) cells were counted in 25 video images recorded and expressed per mm². The adherence counts of nine experiments were averaged. The bars express the percentage of adherent cells when compared with the positive control (i.e., adhesion of untreated neutrophils to stimulated endothelium = 100%). Ac^+Xyl^+, Acetyl- and xylose-containing GXM; Ac^- or Xyl^-, acetyl- or xylose-deficient GXM, respectively. *, $p < 0.05$ when comparing rolling of neutrophils treated with genetically or chemically modified GXM with that of unmodified GXM from the isogenic strain. The error bars represent the SDs.

However, both chemical and genetic deacetylation of GXM abolished the ability of GXM to reduce neutrophil rolling (4% and 5% inhibition, respectively; $p = 1$ in both cases when comparing with untreated neutrophils).

In contrast, GXM lacking xylose (from the $uxs1\Delta$ strain NE178) reduced neutrophil rolling to a comparable extent as xylose-positive GXM of NE167 (Fig. 2; 26% vs 32% inhibition, respectively; $p = 1$).

These results are comparable with those observed in the chemokinesis experiments and indicate that *O*-acetylation, but not xylose, appears to be important for the interference of GXM with neutrophil rolling.

Firm adhesion of neutrophils to stimulated endothelium

In a previous study, we reported that preincubation of neutrophils with GXM led to a considerable reduction in the firm adherence of neutrophils to TNF-α-stimulated endothelium (21).

In the current study, treatment of neutrophils with chemically or genetically deacetylated GXM (isolated from strains ATCC-62066 and NE168, respectively) scarcely affected neutrophil adhesion (Fig. 3; 0–9%) when compared with unmodified GXM derived from the original strains (29–34% inhibition).

In addition, xylose-deficient GXM ($uxs1\Delta$ strain NE178) appeared to be less potent than xylose-positive GXM (NE167) in reducing neutrophil adhesion (inhibition of adhesion 17–18% vs 29–31%, respectively; $p < 0.05$ when comparing both), although the difference was less pronounced as observed for deacetylated GXM.

Thus, in addition to *O*-acetyl, xylose appears to play a modest role in the GXM-related interference with firm neutrophil adhesion in a static model.

In vivo effect of deacetylation on neutrophil influx in myocardial ischemia

Seven animals were subjected to a sham operation. Of the 26 animals that were subjected to coronary artery ligation, 16 animals
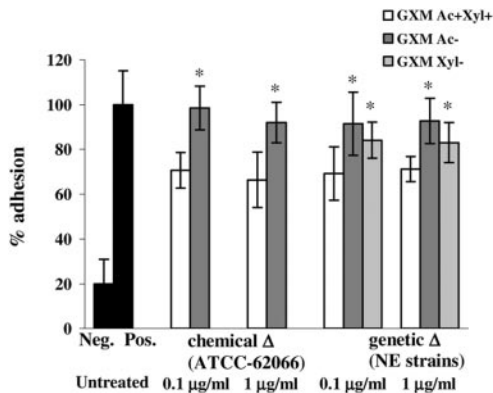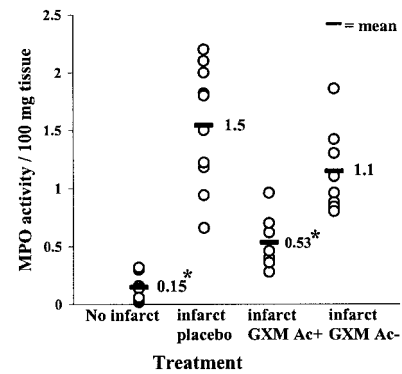

FIGURE 4. Effect of i.v. GXM on MPO content of ischemic myocardium. Rats were subjected to coronary artery ligation (infarct animals) or sham operation (sham animals; $n = 7$) during 1 h followed by a 3-h reperfusion period. Infarct animals received either a placebo (250 μl of normal saline; $n = 10$) or a 2.5-mg bolus of unmodified GXM (GXM Ac$^+$) or de-*O*-acetylated GXM (GXM Ac$^-$) i.v. ($n = 8$ in each group). The hearts were removed at the termination of experiments and the nonperfused (ischemic) area was determined, cut out, and homogenized. MPO content was used as a measure of neutrophil influx and was enzymatically detected in the resulting supernatants. The color development caused by the reaction was detected by spectrophotometry. The *y*-axis expresses the MPO activity as the absorbance change per minute per 100 mg of tissue; the *x*-axis expresses the different treatment groups. *, $p < 0.05$.

were randomly treated with either *O*-acetyl-negative or *O*-acetyl-positive GXM i.v., whereas 10 animals received normal saline (i.e., placebo). The neutrophil accumulation in the dissected ischemic myocardium (i.e., the nonperfused area) was quantified by the detection of tissue MPO. When compared with placebo treatment, the administration of unmodified (acetyl-positive) GXM led to a 65% reduction of MPO activity in the ischemic myocardium, whereas acetyl-negative GXM did not reduce MPO activity significantly (Fig. 4; 23% reduction, $p = 0.6$).

To exclude that a faster clearance of deacetylated GXM from the circulation caused the reduced ability to prevent neutrophil recruitment in the ischemic myocardium, the serum levels of GXM were compared. Serum levels of both *O*-acetyl-negative and *O*-acetyl-positive GXM could be deduced from the separate standard curves that were created for each type of GXM. Serum levels of *O*-acetyl-negative GXM in treated animals were comparable with that of *O*-acetyl-positive GXM (Fig. 5*A*; mean, 130 $\pm$ 42 μg/ml and 118 $\pm$ 30 μg/ml, respectively; $p = 0.4$). For both unmodified GXM and de-*O*-acetylated GXM treatment, a correlation could be demonstrated between the serum concentration of GXM and the degree of MPO reduction (Fig. 5*B*; correlation coefficients -0.45 and -0.68, respectively; two-sided $p < 0.05$).

Complement activation by GXM

GXM-induced complement activation, resulting in the systemic generation of C5a, would theoretically prevent neutrophils from responding properly to other chemoattracting substances present in the inflamed tissues. Although soluble GXM is a poor activator of the complement system, we wanted to exclude the possibility that differences in the generation of (low levels of) C5a might be responsible for the observed differences between wild-type and deacetylated GXM activities in vivo. Here, no significant amounts of C5a could be detected in plasma samples derived from GXM-treated animals (data not shown). However, the inability to detect C5a in these plasma samples might be a consequence of the detection limit of the used assay. Therefore, we assessed the in vitro ability of GXM to generate C5a. In vitro stimulation of control plasma with either unmodified or *O*-acetyl-negative GXM led to a

FIGURE 3. Firm adhesion of GXM-treated neutrophils to endothelium. 2',7'-bis(carboxyethyl)-5(6)-carboxyfluorescein-labeled neutrophils were incubated with GXM (0.1 μg/ml, 37° C, 45 min), followed by adhesion to TNF-α-stimulated HUVEC monolayers in a static adhesion model (see *Materials and Methods*). Adherent neutrophils were counted by fluorescence microscopy and observations were made in quadruplicate. The negative control consisted of the adhesion of untreated neutrophils to unstimulated endothelium, the positive control represents the adhesion of untreated neutrophils to TNF-α-stimulated endothelium. The results of 15 experiments were averaged and subsequently expressed as the percentage of adhesion compared with the positive control (i.e., adhesion of untreated neutrophils to stimulated endothelium = 100%). Negative control, Adhesion of untreated neutrophils to unstimulated HUVECs; positive control, adhesion of untreated neutrophils to TNF-α-stimulated HUVECs; Ac$^+$Xyl$^+$, unmodified GXM containing acetyl and xylose; Ac$^-$ or Xyl$^-$, acetyl- or xylose-deficient GXM. *, $p < 0.05$ when comparing neutrophil treatment with modified GXM with that of unmodified GXM (Ac$^+$Xyl$^+$) from the isogenic strain. The error bars represent the SDs.
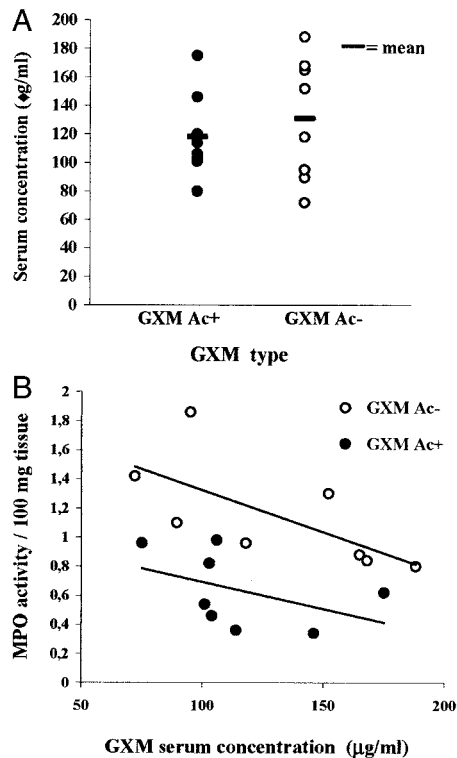
FIGURE 5. Relation of GXM serum concentration to the MPO content of ischemic myocardium. GXM concentrations were measured in serum of rats by a commercial ELISA kit and were calculated from the absorbance data using a standard curve of dilution series for both unmodified and O-acetyl-negative GXM. The MPO activity was determined in the ischemic myocardium of corresponding rats. *A,* Comparison between the serum concentrations of GXM from animals that had received 2.5 mg of either unmodified GXM (GXM Ac^{+}; $n = 8$) or deacetylated GXM (GXM Ac^{-}; $n = 8$). –, Mean. *B,* Inverse correlation between the serum concentration of GXM and the MPO activity in the ischemic myocardium of corresponding rats. The filled dots represent the separate rats treated with O-acetyl-positive GXM and the open dots represent those treated with O-acetyl-negative GXM. The black lines represent the trend lines, which were calculated by linear regression (correlation coefficient: −0.45 and −0.68, respectively; $n = 8$ in both groups; two-sided $p < 0.001$).

dose-dependent generation of (similar levels of) C5a in both cases (Fig. 6). However, at GXM concentrations that were comparable with those detected in animals treated with GXM (80–188 µg/ml), in vitro no or little C5a was generated, especially when compared with zymosan-induced C5a. Notably, when compared with incubation at 4°C, incubation at 37° C in the absence of GXM led to the generation of low levels of C5a (Fig. 6). The addition of GXM to recombinant C5a did not affect stimulation of the C5aR transfectants by C5a alone, which excludes that GXM binds to C5a (data not shown).

Therefore, we concluded that complement activation by GXM plays little or (presumably) no role in the observed interference with neutrophil migration.

Discussion

Previous studies from others and our group on the mechanism of action of GXM have focused on the different stages of neutrophil migration and the identification of GXM-binding receptors. Knowing the importance of the structural epitopes of GXM for the process of neutrophil inhibition will aid the search for specific receptors that are directly involved in the modulating actions of cryptococcal GXM on the host immune response. Studies that used
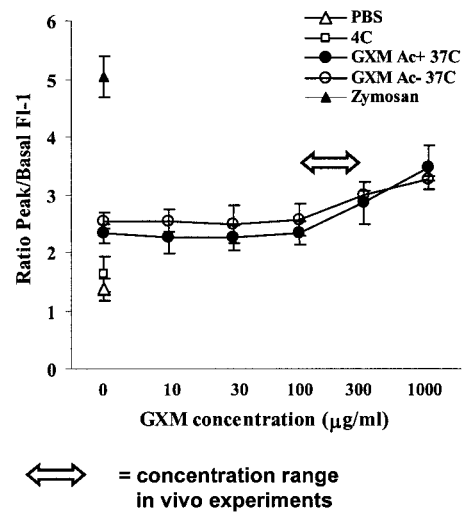

= concentration range in vivo experiments

FIGURE 6. Complement activation by GXM. Plasma of control rats ($n = 4$) was stimulated in vitro at 37°C with increasing concentrations of O-acetyl-positive or O-acetyl-negative GXM. These were compared with the C5a activity in normal saline (PBS), plasma kept at 4°C (4C), plasma stimulated with PBS at 37°C (no GXM), and zymosan-stimulated rat plasma (positive control). The presence of C5a in samples was detected by the ability of C5a to induce a rapid mobilization of calcium in U937-C5aR transfectants loaded with a calcium-specific intracellular probe. The resulting increase in the fluorescent signal was detected by FACS by repetitive measurements during 10 s. The data are expressed as relative values comparing the peak fluorescence to the basal fluorescence value before stimulation (increase in fluorescence = peak value:basal value). The results are the averages of separate stimulations of plasma from four different control rats. Error bars represent the SDs.

chemically or genetically modified GXM have revealed the importance of the individual structural components of GXM for its attribution to virulence.

Here, we investigated the contribution of O-acetylation and xylose to the interference of GXM with the chemokinesis of neutrophils (10, 11, 14) and the process of neutrophil adhesion to the endothelium (20, 21). We compared chemically deacetylated GXM and GXM deficient in either O-acetyl or xylose derived from *cas1*Δ and *uxs1*Δ mutant strains, respectively, with GXM from the corresponding isogenic strains. Deacetylated GXM was considerably less potent than unmodified GXM in interfering with neutrophil chemokinesis toward fMLP, as well as with both phases of neutrophil adhesion. This might be explained by a shared component in the cellular process with which GXM interferes in these different stages of migration (e.g., a common GXM receptor or signaling pathway). Unmodified GXM of strains NE167 and ATCC-62066 inhibited neutrophil migration to a comparable extent while differing in acetyl content (Table II). Apparently, a certain level of O-acetylation is sufficient for the inhibitory effects of GXM. Notably, although Janbon et al. (29) did not detect any O-acetylation on GXM of the *cas1*Δ strain (NE168), we detected 9% O-acetylation. This discrepancy might be caused by the different assays used to determine O-acetylation or, alternatively, by the slightly different purification strategies.

Because de-O-acetylation completely abolished the GXM-related interference with neutrophil rolling and firm adhesion, 6-O-acetyl-D-mannose appears to be a major factor for these functions of GXM. However, deacetylation did not completely abolish GXM-related interference with chemokinesis. Thus, for the interference with chemokinesis, additional factors might play a role. In our experiments, xylosylation of GXM was not important for the

effects on neutrophil chemotaxis or neutrophil rolling, but did appear to play a modest role in the interference with the firm adhesion to endothelium. This indicates that specificity also exists in the cellular pathways after GXM treatment when comparing these different stages in neutrophil migration. Notably, the degree by which xylose-containing GXM inhibited the different migration assays was comparable between unmodified GXM from strains ATCC-62066 and NE167 that differed in (relative) xylose content, which also suggests that the role of xylose will only be modest.

The physicochemical properties of GXM and its deacetylated analog, such as viscosity and size, were similar and therefore do not explain the effect of GXM on chemokinesis and adhesion of neutrophils. Thus, the observed effects appear to be specific and we therefore envisage the existence of a receptor that is crucial for the inhibitory effects of GXM and binds 6-*O*-acetyl-α-D-mannose, possibly as part of a larger saccharide structure.

The importance of *O*-acetylation for the reduction of neutrophil migration by GXM was affirmed in vivo over a concentration range (50–200 μg/ml; Fig. 5*B*) generally observed in patients. Chemical deacetylation considerably reduced the capacity of GXM to diminish neutrophil influx in the injured myocardium in a model of ischemia/reperfusion, whereas serum concentrations of GXM and deacetylated GXM were comparable. Detection of GXM concentration was based on an ELISA system using anti-GXM Abs. Although detection limits for unmodified and deacetylated GXM differed (1 ng/ml vs 100 ng/ml, respectively), concentrations of both could be deduced from the separate standard curves that were created for each type of GXM. The lower reactivity of *O*-acetyl-negative GXM was recognized previously and could be easily explained by the fact that *O*-acetyl is a major binding epitope for polyclonal and many mAbs (22, 26, 27, 31, 32).

In vivo, the generation of C5a due to complement activation by isolated GXM might influence the effects on neutrophil migration. Although poorly, soluble GXM is able to activate complement (57). In line with this paper, we recently obtained evidence that the observed interference with neutrophil migration toward inflammatory sites is not caused by GXM-related complement activation and the subsequent generation of chemotactic C5a (37). In that study, no significant amounts of C5a could be detected in plasma of rats treated with unmodified GXM. Additionally, in vitro stimulation of plasma with GXM at concentrations comparable with those detected in treated animals generated no or little amounts of chemotactic C5a. Here we show that, although different in their effect on neutrophil recruitment, *O*-acetyl-positive and *O*-acetyl-negative GXM induce low levels of C5a to a similar degree. Although pitfalls exist in the detection of C5a (because C5a breaks down rapidly) this observation further supports the hypothesis that the effects of GXM on chemokinesis are complement-independent and rely on direct effects of GXM on neutrophils.

At present, a receptor that binds 6-*O*-acetyl-α-D-mannose, thereby initiating the cellular mechanisms leading to interference with neutrophil chemokinesis and adhesion, remains to be elucidated. *O*-Acetyl groups are common substituents of bacterial polysaccharides and generally determine immune reactivity and function as epitopes for Ab binding; other functions have scarcely been described (58–60). The 6-*O*-acetylated (1→3)-α-D-mannan from *Dictyophora indusiata* has been reported to have anti-inflammatory capacity by unknown mechanisms (61, 62). Additionally, no neutrophil receptors are known to bind *O*-acetylated glycan.

Quite a few carbohydrate structures have been shown to interfere with adhesion by an effect on leukocytes, such as heparin, heparan sulfate (63, 64), fucoidin (a sulfated fucan from algae) (65, 66), and mannose-6-phosphate (67). In most examples, these saccharides share no common structural elements with GXM, and

sulfation or phosphorylation appears essential for their effects. However, smaller nonsulfated or phosphorylated sugars, such as L-fucose, D-mannose, and disaccharides derived from heparin, also affect leukocyte adhesion (67, 68). Although heparin has been shown to bind CD11b/CD18 and P-selectin (69, 70), no specific receptors on leukocytes have been identified for the other carbohydrates. Because TLR4, CD18, and CD14 are potential receptors for GXM (19, 71, 72) and we recently demonstrated that both TLR4 and CD14 play a role in the GXM-related interference with neutrophil rolling (20), additional binding studies using de-*O*-acetylated GXM will reveal whether *O*-acetyl is the major binding epitope for these specific receptors and will reveal the importance of these receptors for the GXM-induced inhibition of neutrophil migration.

In conclusion, we established that *O*-acetyl-mannose is a dominant epitope for the effects of GXM on chemokinesis and endothelial adhesion of neutrophils.

Acknowledgments

References

1. Diamond, R. D., and J. E. Bennett. 1974. Prognostic factors in cryptococcal meningitis. A study in 111 cases. *Ann. Intern. Med. 80:176.*
2. Eng, R. H., E. Bishburg, S. M. Smith, and R. Kapila. 1986. Cryptococcal infections in patients with acquired immune deficiency syndrome. *Am. J. Med. 81:19.*
3. Gordon, M. A., and D. K. Vedder. 1966. Serologic tests in diagnosis and prognosis of cryptococcosis. *J. Am. Med. Assoc. 197:961.*
4. Kozel, T. R., and R. P. Mastroianni. 1976. Inhibition of phagocytosis by cryptococcal polysaccharide: dissociation of the attachment and ingestion phases of phagocytosis. *Infect. Immun. 14:62.*
5. Kozel, T. R., M. A. Wilson, and J. W. Murphy. 1991. Early events in initiation of alternative complement pathway activation by the capsule of *Cryptococcus neoformans. Infect. Immun. 59:3101.*
6. Murphy, J. W., and J. W. Moorhead. 1982. Regulation of cell-mediated immunity in cryptococcosis. I. Induction of specific afferent T suppressor cells by cryptococcal antigen. *J. Immunol. 128:276.*
7. Levitz, S. M., A. Tabuni, H. Kornfeld, C. C. Reardon, and D. T. Golenbock. 1994. Production of tumor necrosis factor α in human leukocytes stimulated by *Cryptococcus neoformans. Infect. Immun. 62:1975.*
8. Retini, C., A. Vecchiarelli, C. Monari, C. Tascini, F. Bistoni, and T. R. Kozel. 1996. Capsular polysaccharide of *Cryptococcus neoformans* induces proinflammatory cytokine release by human neutrophils. *Infect. Immun. 64:2897.*
9. Dong, Z. M., and J. W. Murphy. 1995. Intravascular cryptococcal culture filtrate (CneF) and its major component, glucuronoxylomannan, are potent inhibitors of leukocyte accumulation. *Infect. Immun. 63:770.*
10. Dong, Z. M., and J. W. Murphy. 1995. Effects of the two varieties of *Cryptococcus neoformans* cells and culture filtrate antigens on neutrophil locomotion. *Infect. Immun. 63:2632.*
11. Lipovsky, M. M., G. Gekker, S. Hu, L. C. Ehrlich, A. I. Hoepelman, and P. K. Peterson. 1998. Cryptococcal glucuronoxylomannan induces interleukin (IL)-8 production by human microglia but inhibits neutrophil migration toward IL-8. *J. Infect. Dis. 177:260.*
12. Lipovsky, M. M., L. J. van Elden, A. M. Walenkamp, J. Dankert, and A. I. Hoepelman. 1998. Does the capsule component of the *Cryptococcus neoformans* glucuronoxylomannan impair transendothelial migration of leukocytes in patients with cryptococcal meningitis? *J. Infect. Dis. 178:1231.*
13. Lipovsky, M. M., L. Tsenova, F. E. Coenjaerts, G. Kaplan, R. Cherniak, and A. I. Hoepelman. 2000. Cryptococcal glucuronoxylomannan delays translocation of leukocytes across the blood-brain barrier in an animal model of acute bacterial meningitis. *J. Neuroimmunology 111:10.*
14. Coenjaerts, F. E., A. M. Walenkamp, P. N. Mwinzi, J. Scharringa, H. A. Dekker, J. A. van Strijp, R. Cherniak, and A. I. Hoepelman. 2001. Potent inhibition of neutrophil migration by cryptococcal mannoprotein-4-induced desensitization. *J. Immunol. 167:3988.*
15. Chaka, W., R. Heyderman, I. Gangaidzo, V. Robertson, P. Mason, J. Verhoef, A. Verheul, and A. I. Hoepelman. 1997. Cytokine profiles in cerebrospinal fluid of human immunodeficiency virus-infected patients with cryptococcal meningitis: no leukocytosis despite high interleukin-8 levels. University of Zimbabwe Meningitis Group. *J. Infect. Dis. 176:1633.*
16. Dong, Z. M., and J. W. Murphy. 1993. Mobility of human neutrophils in response to *Cryptococcus neoformans* cells, culture filtrate antigen, and individual components of the antigen. *Infect. Immun. 61:5067.*

17. Monari, C., T. R. Kozel, F. Bistoni, and A. Vecchiarelli. 2002. Modulation of C5aR expression on human neutrophils by encapsulated and acapsular *Cryptococcus neoformans*. *Infect. Immun.* 70:3363.

18. Dong, Z. M., and J. W. Murphy. 1996. Cryptococcal polysaccharides induce L-selectin shedding and tumor necrosis factor receptor loss from the surface of human neutrophils. *J. Clin. Invest.* 97:689.

19. Dong, Z. M., and J. W. Murphy. 1997. Cryptococcal polysaccharides bind to CD18 on human neutrophils. *Infect. Immun.* 65:557.

20. Ellerbroek, P. M., L. H. Ulfman, I. M. Hoepelman, and F. E. J. Coenjaerts. 2004. Cryptococcal glucuronoxylomannan interferes with neutrophil rolling on the endothelium. *Cell. Microbiol.* 6:581.

21. Ellerbroek, P. M., A. I. Hoepelman, F. Wolbers, J. J. Zwaginga, and F. E. Coenjaerts. 2002. Cryptococcal glucuronoxylomannan inhibits adhesion of neutrophils to stimulated endothelium in vitro by affecting both neutrophils and endothelial cells. *Infect. Immun.* 70:4762.

22. Cherniak, R., E. Reiss, M. E. Slodki, R. D. Plattner, and S. O. Blumer. 1980. Structure and antigenic activity of the capsular polysaccharide of *Cryptococcus neoformans* serotype A. *Mol. Immunol.* 17:1025.

23. Small, J. M., T. G. Mitchell, and R. W. Wheat. 1986. Strain variation in composition and molecular size of the capsular polysaccharide of *Cryptococcus neoformans* serotype A. *Infect. Immun.* 54:735.

24. Small, J. M., and T. G. Mitchell. 1989. Strain variation in antiphagocytic activity of capsular polysaccharides from *Cryptococcus neoformans* serotype A. *Infect. Immun.* 57:3751.

25. Young, B. J., and T. R. Kozel. 1993. Effects of strain variation, serotype, and structural modification on kinetics for activation and binding of C3 to *Cryptococcus neoformans*. *Infect. Immun.* 61:2966.

26. Kozel, T. R., and E. C. Gotschlich. 1982. The capsule of *Cryptococcus neoformans* passively inhibits phagocytosis of the yeast by macrophages. *J. Immunol.* 129:1675.

27. Belay, T., and R. Cherniak. 1995. Determination of antigen binding specificities of *Cryptococcus neoformans* factor sera by enzyme-linked immunosorbent assay. *Infect. Immun.* 63:1810.

28. Bar-Peled, M., C. L. Griffith, and T. L. Doering. 2001. Functional cloning and characterization of a UDP-glucuronic acid decarboxylase: the pathogenic fungus *Cryptococcus neoformans* elucidates UDP-xylose synthesis. *Proc. Natl. Acad. Sci. USA* 98:12003.

29. Janbon, G., U. Himmelreich, F. Moyrand, L. Improvisi, and F. Dromer. 2001. Cas1p is a membrane protein necessary for the *O*-acetylation of the *Cryptococcus neoformans* capsular polysaccharide. *Mol. Microbiol.* 42:453.

30. Moyrand, F., B. Klaproth, U. Himmelreich, F. Dromer, and G. Janbon. 2002. Isolation and characterization of capsule structure mutant strains of *Cryptococcus neoformans*. *Mol. Microbiol.* 45:837.

31. Kozel, T. R., S. M. Levitz, F. Dromer, M. A. Gates, P. Thorkildson, and G. Janbon. 2003. Antigenic and biological characteristics of mutant strains of *Cryptococcus neoformans* lacking capsular *O* acetylation or xylosyl side chains. *Infect. Immun.* 71:2868.

32. Eckert, T. F., and T. R. Kozel. 1987. Production and characterization of monoclonal antibodies specific for *Cryptococcus neoformans* capsular polysaccharide. *Infect. Immun.* 55:1895.

33. Washburn, R. G., B. J. Bryant-Varela, N. C. Julian, and J. E. Bennett. 1991. Differences in *Cryptococcus neoformans* capsular polysaccharide structure influence assembly of alternative complement pathway C3 convertase on fungal surfaces. *Mol. Immunol.* 28:465.

34. Sahu, A., T. R. Kozel, and M. K. Pangburn. 1994. Specificity of the thioester-containing reactive site of human C3 and its significance to complement activation. *Biochem. J.* 302(Pt. 2):429.

35. Kozel, T. R., E. Reiss, and R. Cherniak. 1980. Concomitant but not causal association between surface charge and inhibition of phagocytosis by cryptococcal polysaccharide. *Infect. Immun.* 29:295.

36. Kozel, T. R., and C. A. Hermerath. 1984. Binding of cryptococcal polysaccharide to *Cryptococcus neoformans*. *Infect. Immun.* 43:879.

37. Ellerbroek, P. M., R. G. Schoemaker, R. van Veghel, I. M. Hoepelman, and F. E. Coenjaerts. 2004. Cryptococcal capsular glucuronoxylomannan reduces ischemia-related neutrophil influx. *Eur. J. Clin. Invest.* 34:631.

38. Wickes, B. L., and J. C. Edman. 1995. The *Cryptococcus neoformans* GAL7 gene and its use as an inducible promoter. *Mol. Microbiol.* 16:1099.

39. Snippe, H., A. J. van Houte, J. E. van Dam, M. J. De Reuver, M. Jansze, and J. M. Willers. 1983. Immunogenic properties in mice of hexasaccharide from the capsular polysaccharide of *Streptococcus pneumoniae* type 3. *Infect. Immun.* 40:856.

40. Cherniak, R., L. C. Morris, B. C. Anderson, and S. A. Meyer. 1991. Facilitated isolation, purification, and analysis of glucuronoxylomannan of *Cryptococcus neoformans*. *Infect. Immun.* 59:59.

41. Hestrin, S. 1949. The reaction of acetylcholine and other carboxylic acid derivatives with hydroxylamine, and its analytical application. *J. Biol. Chem.* 180:249.

42. Kamerling, J. P., and J. F. G. Vliegenthart. 1989. Mass spectrometry. In *Clinical Biochemistry: Principles, Methods, Applications*, Vol. 1. A. M. Lawson, ed. Walter de Gruyter, Berlin, p. 176.

43. Jaffe, E. A., R. L. Nachman, C. G. Becker, and C. R. Minick. 1973. Culture of human endothelial cells derived from umbilical veins: identification by morphologic and immunologic criteria. *J. Clin. Invest.* 52:2745.

44. Lobb, R. R., G. Chi-Rosso, D. R. Leone, M. D. Rosa, S. Bixler, B. M. Newman, S. Luhowskyj, C. D. Benjamin, I. G. Dougas, and S. E. Goelz. 1991. Expression and functional characterization of a soluble form of endothelial-leukocyte adhesion molecule 1. *J. Immunol.* 147:124.

45. Frevert, C. W., V. A. Wong, R. B. Goodman, R. Goodwin, and T. R. Martin. 1998. Rapid fluorescence-based measurement of neutrophil migration in vitro. *J. Immunol. Methods* 213:41.

46. van Zanten, H., E. U. Saelman, K. M. Schut-Hese, Y. P. Wu, P. J. Slootweg, H. K. Nieuwenhuis, P. G. de Groot, and J. J. Sixma. 1996. Platelet adhesion to collagen type IV under flow conditions. *Blood* 88:3862.

47. Fishbein, M. C., D. Maclean, and P. R. Maroko. 1978. Experimental myocardial infarction in the rat: qualitative and quantitative changes during pathologic evolution. *Am. J. Pathol.* 90:57.

48. Smith, E. F., III, J. W. Egan, P. J. Bugelski, L. M. Hillegass, D. E. Hill, and D. E. Griswold. 1988. Temporal relation between neutrophil accumulation and myocardial reperfusion injury. *Am. J. Physiol.* 255:H1060.

49. Dreyer, W. J., L. H. Michael, M. S. West, C. W. Smith, R. Rothlein, R. D. Rossen, D. C. Anderson, and M. L. Entman. 1991. Neutrophil accumulation in ischemic canine myocardium: insights into time course, distribution, and mechanism of localization during early reperfusion. *Circulation* 84:400.

50. Xia, Y., and J. L. Zweier. 1997. Measurement of myeloperoxidase in leukocyte-containing tissues. *Anal. Biochem.* 245:93.

51. Griswold, D. E., L. M. Hillegass, D. E. Hill, J. W. Egan, and E. F. Smith, III. 1988. Method for quantification of myocardial infarction and inflammatory cell infiltration in rat cardiac tissue. *J. Pharmacol. Methods* 20:225.

52. Bradley, P. P., D. A. Priebat, R. D. Christensen, and G. Rothstein. 1982. Measurement of cutaneous inflammation: estimation of neutrophil content with an enzyme marker. *J. Invest Dermatol.* 78:206.

53. Fearon, D. T., and K. F. Austen. 1977. Activation of the alternative complement pathway due to resistance of zymosan-bound. *Proc. Natl. Acad. Sci. USA* 74:1683.

54. Kew, R. R., T. Peng, S. J. DiMartino, D. Madhavan, S. J. Weinman, D. Cheng, and E. R. Prossnitz. 1997. Undifferentiated U937 cells transfected with chemoattractant receptors: a model system to investigate chemotactic mechanisms and receptor structure/function relationships. *J. Leukocyte Biol.* 61:329.

55. Burchiel, S. W., B. S. Edwards, F. W. Kuckuck, F. T. Lauer, E. R. Prossnitz, J. T. Ransom, and L. A. Sklar. 2000. Analysis of free intracellular calcium by flow cytometry: multiparameter and pharmacologic applications. *Methods* 21:221.

56. Bhattacharjee, A. K., J. E. Bennett, and C. P. Glaudemans. 1984. Capsular polysaccharides of *Cryptococcus neoformans*. *Rev. Infect. Dis.* 6:619.

57. Laxalt, K. A., and T. R. Kozel. 1979. Chemotaxigenesis and activation of the alternative complement pathway by encapsulated and non-encapsulated *Cryptococcus neoformans*. *Infect. Immun.* 26:435.

58. Vodopija, I., Z. Baklaic, P. Hauser, P. Roelants, F. E. Andre, and A. Safary. 1983. Reactivity and immunogenicity of bivalent (AC) and tetravalent (ACW135Y) meningococcal vaccines containing *O*-acetyl-negative or *O*-acetyl-positive group C polysaccharide. *Infect. Immun.* 42:599.

59. Cescutti, P., N. Ravenscroft, S. Ng, Z. Lam, and G. G. Dutton. 1993. Structural investigation of the capsular polysaccharide produced by a novel Klebsiella serotype (SK1): location of *O*-acetyl substituents using NMR and MS techniques. *Carbohydr. Res.* 244:325.

60. Lemercinier, X., I. Martinez-Cabrera, and C. Jones. 2000. Use and validation of an NMR test for the identity and *O*-acetyl content of the Salmonella typhi Vi capsular polysaccharide vaccine. *Biologicals* 28:17.

61. Ukai, S., T. Kiho, C. Hara, I. Kuruma, and Y. Tanaka. 1983. Polysaccharides in fungi. XIV. Anti-inflammatory effect of the polysaccharides from the fruit bodies of several fungi. *J. Pharmacobiodyn.* 6:983.

62. Hara, C., Y. Kumazawa, K. Inagaki, M. Kaneko, T. Kiho, and S. Ukai. 1991. Mitogenic and colony-stimulating factor-inducing activities of polysaccharide fractions from the fruit bodies of *Dictyophora indusiata* Fisch. *Chem. Pharm. Bull. (Tokyo)* 39:1615.

63. Yanaka, K., S. R. Spellman, J. B. McCarthy, T. R. Oegema, Jr., W. C. Low, and P. J. Camarata. 1996. Reduction of brain injury using heparin to inhibit leukocyte accumulation in a rat model of transient focal cerebral ischemia. I. Protective mechanism. *J. Neurosurg.* 85:1102.

64. Lever, R., J. R. Hoult, and C. P. Page. 2000. The effects of heparin and related molecules upon the adhesion of human polymorphonuclear leucocytes to vascular endothelium in vitro. *Br. J. Pharmacol.* 129:533.

65. Stoolman, L. M., and S. D. Rosen. 1983. Possible role for cell-surface carbohydrate-binding molecules in lymphocyte recirculation. *J. Cell Biol.* 96:722.

66. Ley, K., G. Linnemann, M. Meinen, L. M. Stoolman, and P. Gaehtgens. 1993. Fucoidin, but not yeast polyphosphomannan PPME, inhibits leukocyte rolling in venules of the rat mesentery. *Blood* 81:177.

67. Stoolman, L. M., T. S. Tenforde, and S. D. Rosen. 1984. Phosphomannosyl receptors may participate in the adhesive interaction between lymphocytes and high endothelial venules. *J. Cell Biol.* 99:1535.

68. Hershkoviz, R., H. Schor, A. Ariel, I. Hecht, I. R. Cohen, O. Lider, and L. Cahalon. 2000. Disaccharides generated from heparan sulphate or heparin modulate chemokine-induced T-cell adhesion to extracellular matrix. *Immunology* 99:87.

69. Watt, S. M., J. Williamson, H. Genevier, J. Fawcett, D. L. Simmons, A. Hatzfeld, S. A. Nesbitt, and D. R. Coombe. 1993. The heparin binding PECAM-1 adhesion molecule is expressed by CD34$^+$ hematopoietic precursor cells with early myeloid and B-lymphoid cell phenotypes. *Blood* 82:2649.

70. Peter, K., M. Schwarz, C. Conradt, T. Nordt, M. Moser, W. Kubler, and C. Bode. 1999. Heparin inhibits ligand binding to the leukocyte integrin Mac-1 (CD11b/CD18). *Circulation* 100:1533.

71. Shoham, S., C. Huang, J. M. Chen, D. T. Golenbock, and S. M. Levitz. 2001. Toll-like receptor 4 mediates intracellular signaling without TNF-α release in response to *Cryptococcus neoformans* polysaccharide capsule. *J. Immunol.* 166:4620.

72. Monari, C., C. Retini, A. Casadevall, D. Netski, F. Bistoni, T. R. Kozel, and A. Vecchiarelli. 2003. Differences in outcome of the interaction between *Cryptococcus neoformans* glucuronoxylomannan and human monocytes and neutrophils. *Eur. J. Immunol.* 33:1041.